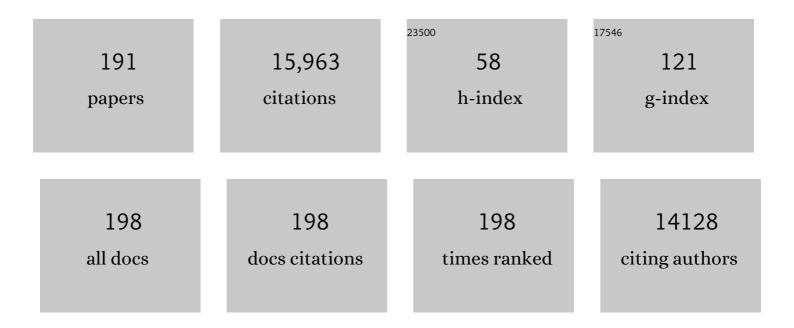
## Yong Wang

List of Publications by Year in descending order

Source: https://exaly.com/author-pdf/6444273/publications.pdf Version: 2024-02-01



#	ARTICLE	IF	CITATIONS
1	Palladium/Ferrierite versus Palladium/SSZâ€13 Passive NOx Adsorbers: Adsorbateâ€Controlled Location of Atomically Dispersed Palladium(II) in Ferrierite Determines High Activity and Stability**. Angewandte Chemie - International Edition, 2022, 61, .	7.2	24
2	Vapor-phase self-assembly for generating thermally stable single-atom catalysts. CheM, 2022, 8, 731-748.	5.8	23
3	Oxidation of Methane to Methanol by Water Over Cu/SSZâ€13: Impact of Cu Loading and Formation of Active Sites. ChemCatChem, 2022, 14, .	1.8	17
4	Elucidating the Role of CO in the NO Storage Mechanism on Pd/SSZ-13 with <i>in Situ</i> DRIFTS. Journal of Physical Chemistry C, 2022, 126, 1439-1449.	1.5	22
5	Noble Metal Singleâ€Atom Catalysts for the Catalytic Oxidation of Volatile Organic Compounds. ChemSusChem, 2022, 15, .	3.6	13
6	ZnAl <sub>2</sub> O <sub>4</sub> Spinel-Supported PdZn <sub>β</sub> Catalyst with Parts per Million Pd for Methanol Steam Reforming. ACS Catalysis, 2022, 12, 2714-2721.	5.5	20
7	Effects of high-temperature CeO <sub>2</sub> calcination on the activity of Pt/CeO <sub>2</sub> catalysts for oxidation of unburned hydrocarbon fuels. Catalysis Science and Technology, 2022, 12, 2462-2470.	2.1	5
8	Noble Metal Singleâ€Atom Catalysts for the Catalytic Oxidation of Volatile Organic Compounds. ChemSusChem, 2022, 15, e202200356.	3.6	4
9	Hydrogen spillover assisted by oxygenate molecules over nonreducible oxides. Nature Communications, 2022, 13, 1457.	5.8	37
10	Shapeâ€Dependent Performance of Cu/Cu <sub>2</sub> O for Photocatalytic Reduction of CO <sub>2</sub> 2. ChemSusChem, 2022, 15, .	3.6	22
11	Coordination environment of active sites and their effect on catalytic performance of heterogeneous catalysts. Chinese Journal of Catalysis, 2022, 43, 928-955.	6.9	23
12	Deactivation by Potassium Accumulation on a Pt/TiO <sub>2</sub> Bifunctional Catalyst for Biomass Catalytic Fast Pyrolysis. ACS Catalysis, 2022, 12, 465-480.	5.5	15
13	Acetone to isobutene conversion on ZnxTiyOz: Effects of TiO2 facet. Journal of Catalysis, 2022, 410, 236-245.	3.1	2
14	Surface Oxygen Vacancies Confined by Ferroelectric Polarization for Tunable CO Oxidation Kinetics. Advanced Materials, 2022, 34, e2202072.	11.1	13
15	Rate Controlling in Low-Temperature Standard NH <sub>3</sub> -SCR: Implications from <i>Operando</i> EPR Spectroscopy and Reaction Kinetics. Journal of the American Chemical Society, 2022, 144, 9734-9746.	6.6	17
16	Selective catalytic reduction of NOx with NH3 over Ce-Mn oxide and Cu-SSZ-13 composite catalysts – Low temperature enhancement. Applied Catalysis B: Environmental, 2022, 316, 121522.	10.8	32
17	Designing Ceria/Alumina for Efficient Trapping of Platinum Single Atoms. ACS Sustainable Chemistry and Engineering, 2022, 10, 7603-7612.	3.2	9
18	Distinct Role of Surface Hydroxyls in Single-Atom Pt <sub>1</sub> /CeO <sub>2</sub> Catalyst for Room-Temperature Formaldehyde Oxidation: Acid–Base Versus Redox. Jacs Au, 2022, 2, 1651-1660.	3.6	25

#	Article	IF	CITATIONS
19	Enhanced Selective Hydrogenolysis of Phenolic C–O Bonds over Graphene-Covered Fe–Co Alloy Catalysts. ACS Sustainable Chemistry and Engineering, 2022, 10, 8588-8596.	3.2	2
20	Reversible transformation between terrace and step sites of Pt nanoparticles on titanium under CO and O2 environments. Chinese Journal of Catalysis, 2022, 43, 2026-2033.	6.9	2
21	Hexagonal boron nitride for selective oxidative dehydrogenation of n-hexane to olefins. Applied Catalysis A: General, 2022, 643, 118763.	2.2	2
22	Remarkable self-degradation of Cu/SAPO-34 selective catalytic reduction catalysts during storage at ambient conditions. Catalysis Today, 2021, 360, 367-374.	2.2	18
23	Conversion of syngas to methanol and DME on highly selective Pd/ZnAl2O4 catalyst. Journal of Energy Chemistry, 2021, 58, 564-572.	7.1	31
24	Selective hydrogenolysis of aryl ether bond over Ru-Fe bimetallic catalyst. Catalysis Today, 2021, 365, 199-205.	2.2	14
25	The superior hydrothermal stability of Pd/SSZ-39 in low temperature passive NOx adsorption (PNA) and methane combustion. Applied Catalysis B: Environmental, 2021, 280, 119449.	10.8	56
26	Atomically Dispersed Dopants for Stabilizing Ceria Surface Area. Applied Catalysis B: Environmental, 2021, 284, 119722.	10.8	37
27	Understanding the Deactivation of Agâ^'ZrO <sub>2</sub> /SiO <sub>2</sub> Catalysts for the Singleâ€step Conversion of Ethanol to Butenes. ChemCatChem, 2021, 13, 999-1008.	1.8	11
28	Elucidation of Active Sites in Aldol Condensation of Acetone over Single-Facet Dominant Anatase TiO <sub>2</sub> (101) and (001) Catalysts. Jacs Au, 2021, 1, 41-52.	3.6	26
29	Economizing on Precious Metals in Threeâ€Way Catalysts: Thermally Stable and Highly Active Singleâ€Atom Rhodium on Ceria for NO Abatement under Dry and Industrially Relevant Conditions**. Angewandte Chemie - International Edition, 2021, 60, 391-398.	7.2	51
30	Economizing on Precious Metals in Threeâ€Way Catalysts: Thermally Stable and Highly Active Singleâ€Atom Rhodium on Ceria for NO Abatement under Dry and Industrially Relevant Conditions**. Angewandte Chemie, 2021, 133, 395-402.	1.6	10
31	High-Field One-Dimensional and Two-Dimensional <sup>27</sup> Al Magic-Angle Spinning Nuclear Magnetic Resonance Study of Î,-, δ-, and γ-Al <sub>2</sub> O <sub>3</sub> Dominated Aluminum Oxides: Toward Understanding the Al Sites in γ-Al <sub>2</sub> O <sub>3</sub> . ACS Omega, 2021, 6, 4090-4099.	1.6	29
32	Controlled Synthesis of Cu <sup>0</sup> /Cu <sub>2</sub> O for Efficient Photothermal Catalytic Conversion of CO <sub>2</sub> and H <sub>2</sub> O. ACS Sustainable Chemistry and Engineering, 2021, 9, 1754-1761.	3.2	53
33	Probing Acid–Base Properties of Anatase TiO <sub>2</sub> Nanoparticles with Dominant {001} and {101} Facets Using Methanol Chemisorption and Surface Reactions. Journal of Physical Chemistry C, 2021, 125, 3988-4000.	1.5	23
34	Onset of High Methane Combustion Rates over Supported Palladium Catalysts: From Isolated Pd Cations to PdO Nanoparticles. Jacs Au, 2021, 1, 396-408.	3.6	37
35	Conversion of ethanol to 1,3–butadiene over Ag–ZrO2/SiO2 catalysts: The role of surface interfaces. Journal of Energy Chemistry, 2021, 54, 7-15.	7.1	21
36	Thermally Stable Singleâ€Atom Heterogeneous Catalysts. Advanced Materials, 2021, 33, e2004319.	11.1	127

#	Article	IF	CITATIONS
37	Elucidation of Active Sites for CH <sub>4</sub> Catalytic Oxidation over Pd/CeO <sub>2</sub> Via Tailoring Metal–Support Interactions. ACS Catalysis, 2021, 11, 5666-5677.	5.5	103
38	Conversion of Formic Acid on Single- and Nano-Crystalline Anatase TiO <sub>2</sub> (101). Journal of Physical Chemistry C, 2021, 125, 7686-7700.	1.5	10
39	Guiding the design of oxidation-resistant Fe-based single atom alloy catalysts with insights from configurational space. Journal of Chemical Physics, 2021, 154, 174709.	1.2	3
40	Critical Role of Al Pair Sites in Methane Oxidation to Methanol on Cu-Exchanged Mordenite Zeolites. Catalysts, 2021, 11, 751.	1.6	4
41	Impact of Hydration on Supported V2O5/TiO2 Catalysts as Explored by Magnetic Resonance Spectroscopy. Journal of Physical Chemistry C, 2021, 125, 16766-16775.	1.5	3
42	Understanding the origin of selective oxidative dehydrogenation of propane on boron-based catalysts. Applied Catalysis A: General, 2021, 623, 118271.	2.2	15
43	The Effect of Pretreatment on the Reactivity of Pd/Al <sub>2</sub> O <sub>3</sub> in Room Temperature Formaldehyde Oxidation. ChemCatChem, 2021, 13, 4133-4141.	1.8	11
44	Recent advances in hybrid metal oxide–zeolite catalysts for low-temperature selective catalytic reduction of NOx by ammonia. Applied Catalysis B: Environmental, 2021, 291, 120054.	10.8	78
45	Elucidating the Cooperative Roles of Water and Lewis Acid–Base Pairs in Cascade C–C Coupling and Self-Deoxygenation Reactions. Jacs Au, 2021, 1, 1471-1487.	3.6	5
46	Unveiling the Interfacial and Structural Heterogeneity of Ti <sub>3</sub> C <sub>2</sub> T <sub><i>x</i></sub> MXene Etched with CoF <sub>2</sub> /HCl by Integrated <i>in Situ</i> Thermal Analysis. ACS Applied Materials & Interfaces, 2021, 13, 52125-52133.	4.0	10
47	Elucidating the Active Site and the Role of Alkali Metals in Selective Hydrodeoxygenation of Phenols over Ironâ€Carbideâ€based Catalyst. ChemSusChem, 2021, 14, 4546-4555.	3.6	8
48	Tailoring the Local Environment of Platinum in Singleâ€Atom Pt <sub>1</sub> /CeO <sub>2</sub> Catalysts for Robust Lowâ€Temperature CO Oxidation. Angewandte Chemie, 2021, 133, 26258-26266.	1.6	7
49	Facet-Dependent selectivity of CeO2 nanoparticles in 2-Propanol conversion. Journal of Catalysis, 2021, 404, 96-108.	3.1	20
50	Toward efficient single-atom catalysts for renewable fuels and chemicals production from biomass and CO2. Applied Catalysis B: Environmental, 2021, 292, 120162.	10.8	114
51	Formation Energetics and Guest—Host Interactions of Molybdenum Carbide Confined in Zeolite Y. Industrial & Engineering Chemistry Research, 2021, 60, 13991-14003.	1.8	3
52	Tailoring the Local Environment of Platinum in Singleâ€Atom Pt <sub>1</sub> /CeO <sub>2</sub> Catalysts for Robust Lowâ€Temperature CO Oxidation. Angewandte Chemie - International Edition, 2021, 60, 26054-26062.	7.2	84
53	Engineering catalyst supports to stabilize PdOx two-dimensional rafts for water-tolerant methane oxidation. Nature Catalysis, 2021, 4, 830-839.	16.1	86
54	Biomimetic CO oxidation below â^'100 °C by a nitrate-containing metal-free microporous system. Nature Communications, 2021, 12, 6033.	5.8	8

#	Article	IF	CITATIONS
55	Frontispiece: Tailoring the Local Environment of Platinum in Singleâ€Atom Pt <sub>1</sub> /CeO <sub>2</sub> Catalysts for Robust Lowâ€Temperature CO Oxidation. Angewandte Chemie - International Edition, 2021, 60, .	7.2	1
56	Frontispiz: Tailoring the Local Environment of Platinum in Singleâ€Atom Pt <sub>1</sub> /CeO <sub>2</sub> Catalysts for Robust Lowâ€Temperature CO Oxidation. Angewandte Chemie, 2021, 133, .	1.6	0
57	Liquid-phase hydrodeoxygenation of lignin-derived phenolics on Pd/Fe: A mechanistic study. Catalysis Today, 2020, 339, 305-311.	2.2	29
58	Influences of Na+ co-cation on the structure and performance of Cu/SSZ-13 selective catalytic reduction catalysts. Catalysis Today, 2020, 339, 233-240.	2.2	40
59	Palladium/Zeolite Low Temperature Passive NOx Adsorbers (PNA): Structure-Adsorption Property Relationships for Hydrothermally Aged PNA Materials. Emission Control Science and Technology, 2020, 6, 126-138.	0.8	38
60	Enhancement of high-temperature selectivity on Cu-SSZ-13 towards NH3-SCR reaction from highly dispersed ZrO2. Applied Catalysis B: Environmental, 2020, 263, 118359.	10.8	42
61	Stabilization of Super Electrophilic Pd <sup>+2</sup> Cations in Small-Pore SSZ-13 Zeolite. Journal of Physical Chemistry C, 2020, 124, 309-321.	1.5	67
62	Coverage-Dependent Adsorption of Phenol on Pt(111) from First Principles. Journal of Physical Chemistry C, 2020, 124, 356-362.	1.5	12
63	Identifying Trends in the Field Ionization of Diatomic Molecules over Adsorbate Covered Pd(331) Surfaces. Topics in Catalysis, 2020, 63, 1510-1521.	1.3	0
64	Single-Step Conversion of Ethanol to <i>n</i> -Butene over Ag-ZrO <sub>2</sub> /SiO <sub>2</sub> Catalysts. ACS Catalysis, 2020, 10, 10602-10613.	5.5	34
65	Low-Temperature Methane Oxidation for Efficient Emission Control in Natural Gas Vehicles: Pd and Beyond. ACS Catalysis, 2020, 10, 14304-14314.	5.5	93
66	Recent Progresses on Structural Reconstruction of Nanosized Metal Catalysts via Controlled-Atmosphere Transmission Electron Microscopy: A Review. ACS Catalysis, 2020, 10, 14419-14450.	5.5	71
67	Direct conversion of methane to formaldehyde and CO on B2O3 catalysts. Nature Communications, 2020, 11, 5693.	5.8	59
68	Hierarchical Echinus-like Cu-MFI Catalysts for Ethanol Dehydrogenation. ACS Catalysis, 2020, 10, 13624-13629.	5.5	63
69	Singleâ€atom Automobile Exhaust Catalysts. ChemNanoMat, 2020, 6, 1659-1682.	1.5	27
70	Reply to: "Pitfalls in identifying active catalyst species― Nature Communications, 2020, 11, 4574.	5.8	0
71	Elucidation of the Active Sites in Single-Atom Pd <sub>1</sub> /CeO <sub>2</sub> Catalysts for Low-Temperature CO Oxidation. ACS Catalysis, 2020, 10, 11356-11364.	5.5	123
72	Quantitative Cu Counting Methodologies for Cu/SSZ-13 Selective Catalytic Reduction Catalysts by Electron Paramagnetic Resonance Spectroscopy. Journal of Physical Chemistry C, 2020, 124, 28061-28073.	1.5	20

Yong Wang

#	Article	IF	CITATIONS
73	Controlling the Oxidation State of Fe-Based Catalysts through Nitrogen Doping toward the Hydrodeoxygenation of <i>m</i> -Cresol. ACS Catalysis, 2020, 10, 7884-7893.	5.5	32
74	Surface engineering of earth-abundant Fe catalysts for selective hydrodeoxygenation of phenolics in liquid phase. Chemical Science, 2020, 11, 5874-5880.	3.7	19
75	CdS/ZnO: A Multipronged Approach for Efficient Reduction of Carbon Dioxide under Visible Light Irradiation. ACS Sustainable Chemistry and Engineering, 2020, 8, 5270-5277.	3.2	70
76	Cu-Exchanged CHA-Type Zeolite from Organic Template-Free Synthesis: An Effective Catalyst for NH <sub>3</sub> -SCR. Industrial & Engineering Chemistry Research, 2020, 59, 7375-7382.	1.8	22
77	Synergetic effect of Lewis acid and base in modified Sn-β on the direct conversion of levoglucosan to lactic acid. Catalysis Science and Technology, 2020, 10, 2986-2993.	2.1	19
78	Probing Active-Site Relocation in Cu/SSZ-13 SCR Catalysts during Hydrothermal Aging by In Situ EPR Spectroscopy, Kinetics Studies, and DFT Calculations. ACS Catalysis, 2020, 10, 9410-9419.	5.5	64
79	Coverage-Dependent Adsorption of Hydrogen on Fe(100): Determining Catalytically Relevant Surface Structures via Lattice Gas Models. Journal of Physical Chemistry C, 2020, 124, 7254-7266.	1.5	15
80	Single-Facet Dominant Anatase TiO <sub>2</sub> (101) and (001) Model Catalysts to Elucidate the Active Sites for Alkanol Dehydration. ACS Catalysis, 2020, 10, 4268-4279.	5.5	32
81	Variable Temperature and Pressure Operando MAS NMR for Catalysis Science and Related Materials. Accounts of Chemical Research, 2020, 53, 611-619.	7.6	48
82	Visualizing H <sub>2</sub> O molecules reacting at TiO <sub>2</sub> active sites with transmission electron microscopy. Science, 2020, 367, 428-430.	6.0	149
83	Recent advances in the selective catalytic hydrodeoxygenation of lignin-derived oxygenates to arenes. Green Chemistry, 2020, 22, 1072-1098.	4.6	130
84	Thermal perturbation of NMR properties in small polar and non-polar molecules. Scientific Reports, 2020, 10, 6097.	1.6	9
85	High-Temperature and High-Pressure In situ Magic Angle Spinning Nuclear Magnetic Resonance Spectroscopy. Journal of Visualized Experiments, 2020, , .	0.2	5
86	An Environmental Transmission Electron Microscopy Study of the Stability of the TiO <sub>2</sub> (1) Tj ETQq(	) 0 0 rgBT	/Overlock 10
87	Mechanism by which Tungsten Oxide Promotes the Activity of Supported V <sub>2</sub> O <sub>5</sub> /TiO <sub>2</sub> Catalysts for NO <sub><i>X</i></sub> Abatement: Structural Effects Revealed by <sup>51</sup> V MAS NMR Spectroscopy. Angewandte Chemie - International Edition. 2019. 58. 12609-12616.	7.2	96
88	Mechanism by which Tungsten Oxide Promotes the Activity of Supported V <sub>2</sub> O <sub>5</sub> /TiO <sub>2</sub> Catalysts for NO <sub><i>X</i></sub> Abatement: Structural Effects Revealed by <sup>51</sup> V MAS NMR Spectroscopy. Angewandte Chemie, 2019, 131,	1.6	45

	12739-12746.			
89	Inhibition of AlF <sub>3</sub> ·3H <sub>2</sub> O Impurity Formation in Ti <sub>3</sub> C <sub>2</sub> T <sub><i>x</i></sub> MXene Synthesis under a Unique CoF <sub><i>x</i></sub> /HCl Etching Environment. ACS Applied Energy Materials, 2019, 2, 8145-8152.	2.5	39	

90Oxidative esterification of acetol with methanol to methyl pyruvate over hydroxyapatite supported<br/>gold catalyst: Essential roles of acid-base properties. Chinese Journal of Catalysis, 2019, 40, 1810-1819.6.910

#	Article	IF	CITATIONS
91	Adsorption and Reaction of Methanol on Anatase TiO <sub>2</sub> (101) Single Crystals and Faceted Nanoparticles. Journal of Physical Chemistry C, 2019, 123, 24133-24145.	1.5	14
92	Revisiting effects of alkali metal and alkaline earth co-cation additives to Cu/SSZ-13 selective catalytic reduction catalysts. Journal of Catalysis, 2019, 378, 363-375.	3.1	59
93	Controllable in Situ Surface Restructuring of Cu Catalysts and Remarkable Enhancement of Their Catalytic Activity. ACS Catalysis, 2019, 9, 2213-2221.	5.5	53
94	Genesis and Stability of Hydronium Ions in Zeolite Channels. Journal of the American Chemical Society, 2019, 141, 3444-3455.	6.6	119
95	Benchmarking the accuracy of coverage-dependent models: adsorption and desorption of benzene on Pt (1 1 1) and Pt3Sn (1 1 1) from first principles. Progress in Surface Science, 2019, 94, 100538.	3.8	10
96	Tuning Ni/Al Ratio to Enhance Pseudocapacitive Charge Storage Properties of Nickel–Aluminum Layered Double Hydroxide. Advanced Electronic Materials, 2019, 5, 1900215.	2.6	39
97	Carbon vacancy defect-activated Pt cluster for hydrogen generation. Journal of Materials Chemistry A, 2019, 7, 15364-15370.	5.2	57
98	Nitrogenâ€Doped Porous Carbon Supported Nonprecious Metal Singleâ€Atom Electrocatalysts: from Synthesis to Application. Small Methods, 2019, 3, 1900159.	4.6	218
99	Tuning Pt-CeO2 interactions by high-temperature vapor-phase synthesis for improved reducibility of lattice oxygen. Nature Communications, 2019, 10, 1358.	5.8	302
100	Unraveling the mysterious failure of Cu/SAPO-34 selective catalytic reduction catalysts. Nature Communications, 2019, 10, 1137.	5.8	99
101	Propane oxidative dehydrogenation over highly selective hexagonal boron nitride catalysts: The role of oxidative coupling of methyl. Science Advances, 2019, 5, eaav8063.	4.7	80
102	Stabilizing High Metal Loadings of Thermally Stable Platinum Single Atoms on an Industrial Catalyst Support. ACS Catalysis, 2019, 9, 3978-3990.	5.5	233
103	The partial reduction of clean and doped α-Fe2O3(0001) from first principles. Applied Catalysis A: General, 2019, 582, 116989.	2.2	6
104	Catalytic activation of ethylene C–H bonds on uniform d <sup>8</sup> Ir( <scp>i</scp> ) and Ni( <scp>ii</scp> ) cations in zeolites: toward molecular level understanding of ethylene polymerization on heterogeneous catalysts. Catalysis Science and Technology, 2019, 9, 6570-6576.	2.1	20
105	Hydrothermally stable ZnAl <sub>2</sub> O <sub>4</sub> nanocrystals with controlled surface structures for the design of long-lasting and highly active/selective PdZn catalysts. Green Chemistry, 2019, 21, 6574-6578.	4.6	7
106	Catalysis with Two-Dimensional Materials Confining Single Atoms: Concept, Design, and Applications. Chemical Reviews, 2019, 119, 1806-1854.	23.0	745
107	Palladium/Beta zeolite passive NOx adsorbers (PNA): Clarification of PNA chemistry and the effects of CO and zeolite crystallite size on PNA performance. Applied Catalysis A: General, 2019, 569, 141-148.	2.2	81
108	Mechanistic insight into the passive NOx adsorption in the highly dispersed Pd/HBEA zeolite. Applied Catalysis A: General, 2019, 569, 181-189.	2.2	55

#	Article	IF	CITATIONS
109	Steam reforming of simulated bio-oil on K-Ni-Cu-Mg-Ce-O/Al2O3: The effect of K. Catalysis Today, 2019, 323, 183-190.	2.2	19
110	Hydrothermal Catalytic Deoxygenation of Fatty Acid and Bio-oil with In Situ H <sub>2</sub> . ACS Sustainable Chemistry and Engineering, 2018, 6, 4521-4530.	3.2	40
111	Modeling the adsorbate coverage distribution over a multi-faceted catalytic grain in the presence of an electric field: O/Fe from first principles. Catalysis Today, 2018, 312, 92-104.	2.2	4
112	Identifying the Thermal Decomposition Mechanism of Guaiacol on Pt(111): An Integrated X-ray Photoelectron Spectroscopy and Density Functional Theory Study. Journal of Physical Chemistry C, 2018, 122, 4261-4273.	1.5	5
113	Mechanistic Effects of Water on the Fe-Catalyzed Hydrodeoxygenation of Phenol. The Role of BrÃ,nsted Acid Sites. ACS Catalysis, 2018, 8, 2200-2208.	5.5	50
114	Molecular Level Understanding of How Oxygen and Carbon Monoxide Improve NO <sub><i>x</i></sub> Storage in Palladium/SSZ-13 Passive NO <sub><i>x</i></sub> Adsorbers: The Role of NO <sup>+</sup> and Pd(II)(CO)(NO) Species. Journal of Physical Chemistry C, 2018, 122, 10820-10827.	1.5	101
115	Ethanol Partial Oxidation over VO <sub><i>x</i></sub> /TiO <sub>2</sub> Catalysts: The Role of Titania Surface Oxygen on Vanadia Reoxidation in the Mars–van Krevelen Mechanism. ACS Catalysis, 2018, 8, 4681-4693.	5.5	33
116	Achieving Atomic Dispersion of Highly Loaded Transition Metals in Smallâ€Pore Zeolite SSZâ€13: Highâ€Capacity and Highâ€Efficiency Lowâ€Temperature CO and Passive NO <sub><i>x</i></sub> Adsorbers. Angewandte Chemie - International Edition, 2018, 57, 16672-16677.	7.2	129
117	Achieving Atomic Dispersion of Highly Loaded Transition Metals in Smallâ€Pore Zeolite SSZâ€13: Highâ€Capacity and Highâ€Efficiency Lowâ€Temperature CO and Passive NO <sub><i>x</i></sub> Adsorbers. Angewandte Chemie, 2018, 130, 16914-16919.	1.6	34
118	Enhanced Antioxidation Stability of Iron-Based Catalysts via Surface Decoration with ppm Platinum. ACS Sustainable Chemistry and Engineering, 2018, 6, 14010-14016.	3.2	13
119	Atom trapping: a novel approach to generate thermally stable and regenerable single-atom catalysts. National Science Review, 2018, 5, 630-632.	4.6	47
120	Correlating DFT Calculations with CO Oxidation Reactivity on Ga-Doped Pt/CeO <sub>2</sub> Single-Atom Catalysts. Journal of Physical Chemistry C, 2018, 122, 22460-22468.	1.5	91
121	Role of Active Phase in Fischer–Tropsch Synthesis: Experimental Evidence of CO Activation over Single-Phase Cobalt Catalysts. ACS Catalysis, 2018, 8, 7787-7798.	5.5	110
122	Propane ammoxidation over MoVTeNb oxide catalyst in a microchannel reactor. AICHE Journal, 2018, 64, 4002-4008.	1.8	11
123	Predicting the Electric Field Effect on the Lateral Interactions Between Adsorbates: O/Fe(100) from First Principles. Topics in Catalysis, 2018, 61, 763-775.	1.3	11
124	In Situ STEM Determination of the Atomic Structure and Reconstruction Mechanism of the TiO <sub>2</sub> (001) (1 Å— 4) Surface. Chemistry of Materials, 2017, 29, 3189-3194.	3.2	40
125	Investigation of Silica-Supported Vanadium Oxide Catalysts by High-Field <sup>51</sup> V Magic-Angle Spinning NMR. Journal of Physical Chemistry C, 2017, 121, 6246-6254.	1.5	39
126	Stabilization and transformation of Pt nanocrystals supported on ZnAl2O4spinel. RSC Advances, 2017, 7, 3282-3286.	1.7	7

#	Article	IF	CITATIONS
127	Fabrication and thermal stability of NH 4 HF 2 -etched Ti 3 C 2 MXene. Ceramics International, 2017, 43, 6322-6328.	2.3	208
128	Stabilization of Iron-Based Catalysts against Oxidation: An <i>In Situ</i> Ambient-Pressure X-ray Photoelectron Spectroscopy (AP-XPS) Study. ACS Catalysis, 2017, 7, 3639-3643.	5.5	36
129	Elucidation of reaction mechanism for m-cresol hydrodeoxygenation over Fe based catalysts: A kinetic study. Catalysis Communications, 2017, 100, 43-47.	1.6	17
130	Catalysts for Steam Reforming of Bio-oil: A Review. Industrial & Engineering Chemistry Research, 2017, 56, 4627-4637.	1.8	139
131	Recent advance in MXenes: A promising 2D material for catalysis, sensor and chemical adsorption. Coordination Chemistry Reviews, 2017, 352, 306-327.	9.5	484
132	Direct Coupling of Thermo―and Photocatalysis for Conversion of CO <sub>2</sub> –H <sub>2</sub> O into Fuels. ChemSusChem, 2017, 10, 4709-4714.	3.6	53
133	Toward Rational Design of Cu/SSZ-13 Selective Catalytic Reduction Catalysts: Implications from Atomic-Level Understanding of Hydrothermal Stability. ACS Catalysis, 2017, 7, 8214-8227.	5.5	278
134	A Strategy for the Simultaneous Synthesis of Methallyl Alcohol and Diethyl Acetal with Snâ $\in \hat{I}^2$ . ChemSusChem, 2017, 10, 4715-4724.	3.6	13
135	Low-Temperature Pd/Zeolite Passive NO <sub><i>x</i></sub> Adsorbers: Structure, Performance, and Adsorption Chemistry. Journal of Physical Chemistry C, 2017, 121, 15793-15803.	1.5	178
136	One-Pot Production of Lactic Acid from Acetol over Dealuminated Sn-Beta Supported Gold Catalyst. ACS Catalysis, 2017, 7, 6038-6047.	5.5	31
137	A Strategy for the Simultaneous Synthesis of Methallyl Alcohol and Diethyl Acetal with Sn-β. ChemSusChem, 2017, 10, 4667-4667.	3.6	0
138	Activation of surface lattice oxygen in single-atom Pt/CeO <sub>2</sub> for low-temperature CO oxidation. Science, 2017, 358, 1419-1423.	6.0	1,114
139	Sub-micron Cu/SSZ-13: Synthesis and application as selective catalytic reduction (SCR) catalysts. Applied Catalysis B: Environmental, 2017, 201, 461-469.	10.8	101
140	Perspective on Catalytic Hydrodeoxygenation of Biomass Pyrolysis Oils: Essential Roles of Fe-Based Catalysts. Catalysis Letters, 2016, 146, 1621-1633.	1.4	42
141	Thermally stable single-atom platinum-on-ceria catalysts via atom trapping. Science, 2016, 353, 150-154.	6.0	1,487
142	The effect of ZnO addition on H2O activation over Co/ZrO2 catalysts. Catalysis Today, 2016, 269, 140-147.	2.2	2
143	Investigating the Surface Structure of γ-Al <sub>2</sub> O <sub>3</sub> Supported WO <sub>X</sub> Catalysts by High Field <sup>27</sup> Al MAS NMR and Electronic Structure Calculations. Journal of Physical Chemistry C, 2016, 120, 23093-23103.	1.5	26
144	Nitrogen-doped flower-like porous carbon materials directed by in situ hydrolysed MgO: Promising support for Ru nanoparticles in catalytic hydrogenations. Nano Research, 2016, 9, 3129-3140.	5.8	24

#	Article	IF	CITATIONS
145	Real-Time Observation of Reconstruction Dynamics on TiO <sub>2</sub> (001) Surface under Oxygen via an Environmental Transmission Electron Microscope. Nano Letters, 2016, 16, 132-137.	4.5	109
146	Adsorption of guaiacol on Fe (110) and Pd (111) from first principles. Surface Science, 2016, 648, 227-235.	0.8	36
147	High field 27Al MAS NMR and TPD studies of active sites in ethanol dehydration using thermally treated transitional aluminas as catalysts. Journal of Catalysis, 2016, 336, 85-93.	3.1	47
148	Hydrothermal catalytic deoxygenation of palmitic acid over nickel catalyst. Fuel, 2016, 166, 302-308.	3.4	110
149	Effect of Water on Ethanol Conversion over ZnO. Topics in Catalysis, 2016, 59, 37-45.	1.3	24
150	Effect of ZnO facet on ethanol steam reforming over Co/ZnO. Catalysis Communications, 2016, 73, 93-97.	1.6	22
151	Effect of Cobalt Particle Size on Acetone Steam Reforming. ChemCatChem, 2015, 7, 2932-2936.	1.8	12
152	Nanocrystalline Anatase Titania-Supported Vanadia Catalysts: Facet-Dependent Structure of Vanadia. Journal of Physical Chemistry C, 2015, 119, 15094-15102.	1.5	28
153	New insights into reaction mechanisms of ethanol steam reforming on Co–ZrO2. Applied Catalysis B: Environmental, 2015, 162, 141-148.	10.8	67
154	Investigation of the Structure and Active Sites of TiO <sub>2</sub> Nanorod Supported VO <sub><i>x</i></sub> Catalysts by High-Field and Fast-Spinning <sup>51</sup> V MAS NMR. ACS Catalysis, 2015, 5, 3945-3952.	5.5	51
155	Effect of Oxygen Defects on the Catalytic Performance of VO <sub><i>x</i></sub> /CeO <sub>2</sub> Catalysts for Oxidative Dehydrogenation of Methanol. ACS Catalysis, 2015, 5, 3006-3012.	5.5	96
156	Hierarchically structured catalysts for cascade and selective steam reforming/hydrodeoxygenation reactions. Chemical Communications, 2015, 51, 16617-16620.	2.2	8
157	Adsorption of aromatics on the (111) surface of PtM and PtM <sub>3</sub> (M = Fe, Ni) alloys. RSC Advances, 2015, 5, 85705-85719.	1.7	14
158	Phenol Deoxygenation Mechanisms on Fe(110) and Pd(111). ACS Catalysis, 2015, 5, 523-536.	5.5	116
159	Low-temperature aqueous-phase reforming of ethanol on bimetallic PdZn catalysts. Catalysis Science and Technology, 2015, 5, 254-263.	2.1	24
160	Sorption-enhanced synthetic natural gas (SNG) production from syngas: A novel process combining CO methanation, water-gas shift, and CO2 capture. Applied Catalysis B: Environmental, 2014, 144, 223-232.	10.8	59
161	Recent Advances in Catalytic Conversion of Ethanol to Chemicals. ACS Catalysis, 2014, 4, 1078-1090.	5.5	494
162	Supported metal catalysts for alcohol/sugar alcohol steam reforming. Dalton Transactions, 2014, 43, 11782.	1.6	60

#	Article	IF	CITATIONS
163	Catalytic fast pyrolysis of lignocellulosic biomass. Chemical Society Reviews, 2014, 43, 7594-7623.	18.7	864
164	Synergistic Catalysis between Pd and Fe in Gas Phase Hydrodeoxygenation of <i>m</i> -Cresol. ACS Catalysis, 2014, 4, 3335-3345.	5.5	173
165	Enhanced Fe <sub>2</sub> O <sub>3</sub> Reducibility via Surface Modification with Pd: Characterizing the Synergy within Pd/Fe Catalysts for Hydrodeoxygenation Reactions. ACS Catalysis, 2014, 4, 3381-3392.	5.5	114
166	Adsorption of phenol on Fe (110) and Pd (111) from first principles. Surface Science, 2014, 630, 244-253.	0.8	52
167	A review on ex situ catalytic fast pyrolysis of biomass. Frontiers of Chemical Science and Engineering, 2014, 8, 280-294.	2.3	103
168	The effect of ZnO addition on Co/C catalyst for vapor and aqueous phase reforming of ethanol. Catalysis Today, 2014, 233, 38-45.	2.2	25
169	Influence of ZnO Facets on Pd/ZnO Catalysts for Methanol Steam Reforming. ACS Catalysis, 2014, 4, 2379-2386.	5.5	99
170	Carbon-supported bimetallic Pd–Fe catalysts for vapor-phase hydrodeoxygenation of guaiacol. Journal of Catalysis, 2013, 306, 47-57.	3.1	384
171	Tailoring the Adsorption of Benzene on PdFe Surfaces: A Density Functional Theory Study. Journal of Physical Chemistry C, 2013, 117, 24317-24328.	1.5	45
172	Stable platinum nanoparticles on specific MgAl2O4 spinel facets at high temperatures in oxidizing atmospheres. Nature Communications, 2013, 4, 2481.	5.8	166
173	Minimizing the Formation of Coke and Methane on Co Nanoparticles in Steam Reforming of Biomassâ€Derived Oxygenates. ChemCatChem, 2013, 5, 1299-1303.	1.8	34
174	Recent Advances in Hydrotreating of Pyrolysis Bio-Oil and Its Oxygen-Containing Model Compounds. ACS Catalysis, 2013, 3, 1047-1070.	5.5	585
175	High CO2 Selectivity of ZnO Powder Catalysts for Methanol Steam Reforming. Journal of Physical Chemistry C, 2013, 117, 6493-6503.	1.5	27
176	Effect of Sodium on the Catalytic Properties of VO <sub><i>x</i></sub> /CeO <sub>2</sub> Catalysts for Oxidative Dehydrogenation of Methanol. Journal of Physical Chemistry C, 2013, 117, 5722-5729.	1.5	25
177	A large sample volume magic angle spinning nuclear magnetic resonance probe for in situ investigations with constant flow of reactants. Physical Chemistry Chemical Physics, 2012, 14, 2137-2143.	1.3	20
178	Bimetallic catalysts for hydrogen generation. Chemical Society Reviews, 2012, 41, 7994.	18.7	309
179	Catalytic reactivity of face centered cubic PdZnα for the steam reforming of methanol. Journal of Catalysis, 2012, 291, 44-54.	3.1	46
180	Catalytic Roles of Co <sup>0</sup> and Co <sup>2+</sup> during Steam Reforming of Ethanol on Co/MgO Catalysts. ACS Catalysis, 2011, 1, 279-286.	5.5	98

#	Article	IF	CITATIONS
181	Direct Conversion of Bio-ethanol to Isobutene on Nanosized Zn <sub><i>x</i></sub> Zr <sub><i>y</i></sub> O <sub><i>z</i></sub> Mixed Oxides with Balanced Acid–Base Sites. Journal of the American Chemical Society, 2011, 133, 11096-11099.	6.6	225
182	The Effect of Zinc Addition on the Oxidation State of Cobalt in Co/ZrO <sub>2</sub> Catalysts. ChemSusChem, 2011, 4, 1679-1684.	3.6	36
183	A comparative study between Co and Rh for steam reforming of ethanol. Applied Catalysis B: Environmental, 2010, 96, 441-448.	10.8	77
184	Aerosol-Derived Bimetallic Alloy Powders: Bridging the Gap. Journal of Physical Chemistry C, 2010, 114, 17181-17190.	1.5	33
185	Intensified Fischer–Tropsch synthesis process with microchannel catalytic reactors. Catalysis Today, 2009, 140, 149-156.	2.2	112
186	Oxidation of ethanol to acetaldehyde over Na-promoted vanadium oxide catalysts. Applied Catalysis A: General, 2007, 332, 263-272.	2.2	36
187	Review of Developments in Portable Hydrogen Production Using Microreactor Technology. Chemical Reviews, 2004, 104, 4767-4790.	23.0	354
188	Methanol steam reforming over Pd/ZnO: Catalyst preparation and pretreatment studies. Fuel Processing Technology, 2003, 83, 193-201.	3.7	93
189	Steam reforming of methanol over highly active Pd/ZnO catalyst. Catalysis Today, 2002, 77, 79-88.	2.2	245
190	Pd/FER vs Pd/SSZâ€13 Passive NOx Adsorbers: Adsorbateâ€controlled Location of Atomically Dispersed Pd(II) in FER Determines High Activity and Stability. Angewandte Chemie, 0, , .	1.6	2
191	Modelling complex molecular interactions in catalytic materials for energy storage and conversion in nuclear magnetic resonance. Frontiers in Catalysis, 0, 2	1.8	1